

DPD-fVAE: Synthetic Data Generation Using Federated Variational Autoencoders With Differentially-Private Decoder

Bjarne Pfitzner and Bert Arnrich

Hasso Plattner Institute

Rudolf-Breitscheid-Str. 187, 14482 Potsdam, Germany

bjarne.pfitzner@hpi.de and bert.arnrich@hpi.de

Abstract

Federated learning (FL) is getting increased attention for processing sensitive, distributed datasets common to domains such as healthcare. Instead of directly training classification models on these datasets, recent works have considered training data generators capable of synthesising a new dataset which is not protected by any privacy restrictions. Thus, the synthetic data can be made available to anyone, which enables further evaluation of machine learning architectures and research questions off-site. As an additional layer of privacy-preservation, differential privacy can be introduced into the training process. We propose DPD-fVAE, a federated Variational Autoencoder with Differentially-Private Decoder, to synthesise a new, labelled dataset for subsequent machine learning tasks. By synchronising only the decoder component with FL, we can reduce the privacy cost per epoch and thus enable better data generators. In our evaluation on MNIST, Fashion-MNIST and CelebA, we show the benefits of DPD-fVAE and report competitive performance to related work in terms of Fréchet Inception Distance and accuracy of classifiers trained on the synthesised dataset.

1. Introduction

The recent advances in machine learning (ML) resulted in an ever-growing number of powerful model architectures to gain knowledge from large-scale datasets. The complexity of many of these (deep) models generally requires a considerable amount of data. While sufficiently large datasets for ML are often theoretically available, they are in practice widely distributed and subject to privacy regulations, such as Europe’s General Data Protection Regulation (GDPR) or the American Health Insurance Portability and Accountability Act (HIPAA). An example of an ML research field suffering from these restrictions is the healthcare domain, where patient data is particularly hard to access for non-

clinical researchers. Moreover, analysing data from different sources except just one is often vital for the validation of ML models to prove the applicability to different data distributions occurring in real life.

Federated learning (FL) has been proposed as a means to train ML models on distributed datasets [37]. It is based on an exchange and averaging of model parameters or parameter updates instead of the actual data. That allows training participants, such as hospitals, to contribute to ML research with their data, without having to transfer it off-site.

However, it has previously been shown that FL alone is not sufficient to guarantee the privacy of sensitive data [24, 39, 52, 57]. By inspecting the model weights or model updates, adversaries can infer information about the underlying data or even reconstruct it. In order to provide training participants with formal guarantees regarding their data’s privacy, many papers adopted differential privacy (DP) along with FL. It describes the introduction of noise into the model, which hides the impact of clients and their individual data on the trained model. In the context of distributed model training, algorithms can either use central differential privacy (CDP), which protects the data on a user level [18, 38] and hides any clients’ participation in the training process, or local differential privacy (LDP), where every individual data point is protected [1].

While FL of classification models has been explored extensively in the literature, training of generative models is not as widely researched so far. Setting up an FL system in real-life can be hard due to a large organisational and legal overhead, as well as necessary data preprocessing steps that allow the same model to be trained by each participant. It is therefore in many cases beneficial to make use of this lengthy and complicated setup phase to train a data generator instead of a classifier. The synthetic data can subsequently be used to analyse several different ML model architectures, whereas using FL for training a classifier directly may only allow one architecture to be evaluated. Moreover, a data generator can be distributed to many researchers that may have different research questions about

the dataset, which have not been considered before. Finally, conditional data generators can augment and balance out imbalanced real datasets with class or property biases that are common in many domains.

In this work, we focus on training variational autoencoders (VAEs) on image datasets in an FL fashion. VAEs are capable of generating new, unseen data by learning a continuous, regular latent space representation of the training data and sampling from it [29]. Synthesis of samples from specific classes is made possible by including the original class labels as a conditional into the model.

Using DP for FL has been shown to be hard, depending on the number of clients and amount of data, since tight privacy bounds require a lot of added noise [3, 4]. We propose a way of reducing the required noise by only training the decoder component of the VAE using DP. This affects the L_2 -norms of client updates, leading to a reduced noise requirement with the same privacy spending.

Our contributions are the following: (i) We propose an altered FL approach for VAEs, named federated Variational Autoencoder with Differentially-Private Decoder (DPD-fVAE), which keeps the encoder component private and user-specific while synchronising only the decoder with DP. (ii) We motivate our method by discussing the interaction of DP hyperparameters and their impact on added noise and model performance. (iii) We evaluate the effectiveness of our approach for non-private FL, as well as FL with central and local DP.

The remainder of this paper is structured as follows. In Sec. 2, we introduce VAEs, FL and DP and Sec. 3 discusses related work. We explain our proposed DPD-fVAE algorithm in Sec. 4. The implementation details, our experimental evaluation and the results are illustrated and discussed in Sec. 5. Finally, Sec. 6 concludes this paper and highlights future work.

2. Preliminaries

2.1. Variational Autoencoders

VAEs [29] are neural network-based generative models consisting of two components: an encoder E , responsible for encoding an input into some latent space distribution, and a decoder D which reconstructs the input based on the latent information [19]. Conditional VAEs additionally take label information into account when encoding and decoding an input.

The encoder provides an approximate posterior distribution of the latent variable z , $q_{\theta_E}(z|\mathbf{x}, y)$, while the decoder aims to reconstruct the original data (\mathbf{x}, y) from the sampled latent space using variational inference, thus maximising the data log-likelihood $\log p_{\theta_D}(\mathbf{x}|y)$. As a proxy for optimising the log-likelihood, VAEs use the Evidence Lower Bound (ELBO), which includes the Kullback-Leibler diver-

gence (KLD) between the approximate posterior and the prior $p(z|y)$ of the latent variable.

In our experiments, we use the recently proposed β -VAE [23], which introduces a weight parameter into the loss function to adjust the impact of the KLD term. The loss \mathcal{L}_β consists of the reconstruction loss \mathcal{L}_{RE} , which is optimised during training, and the KL-loss \mathcal{L}_{KL} , which is used as a regularisation term:

$$\mathcal{L}_\beta = \mathcal{L}_{RE} - \beta \mathcal{L}_{KL}, \quad \text{with} \quad (1)$$

$$\mathcal{L}_{RE} = \mathbb{E}_{q_{\theta_E}} \log p_{\theta_D}(\mathbf{x}|z, y) \quad (2)$$

$$\mathcal{L}_{KL} = \text{KL}(q_{\theta_E}(z|\mathbf{x}, y) || p(z|y)) \quad (3)$$

2.2. Federated Learning

FL was recently introduced as a way to train ML models on distributed datasets without requiring direct data access [37]. Instead, data owners are responsible for training the model on their data and sending model updates, while a central parameter server aggregates these updates from the participants and applies them to the global model.

In detail, an ML model is trained over a number of global rounds, in which the following three steps are repeated: First, the server selects a subset of clients to participate in the current round and sends them the current model weights stored by the server. Second, the chosen clients train the model on their local datasets for a number of epochs and send the weight differences between their own and the global model back to the server. Finally, the server aggregates the received weight updates and applies the update to the global model. A common aggregation strategy is performing a weighted average over the updates, considering the amount of local data each client possesses. The three steps are repeated until convergence of for T rounds.

2.3. Differential Privacy

DP was previously used mainly in the database domain to quantify the privacy leakage from repeated queries on the same dataset. The goal of DP is to add sufficient noise to the queries such that there is plausible deniability that any one data sample is included in the database and contributed to the query results. Formally, (ϵ, δ) -DP is defined as follows:

Definition 1 ((ϵ, δ) -DP [14]) *A randomised mechanism $\mathcal{M} : \mathcal{D} \rightarrow \mathcal{R}$ with domain \mathcal{D} and range \mathcal{R} satisfies (ϵ, δ) -DP if for any two adjacent inputs $d, d' \in \mathcal{D}$ and for any subset of outputs $\mathcal{S} \subseteq \mathcal{R}$ it holds that,*

$$\Pr[\mathcal{M}(d) \in \mathcal{S}] \leq e^\epsilon \Pr[\mathcal{M}(d') \in \mathcal{S}] + \delta \quad (4)$$

Adjacent inputs are defined as differing by only the presence/absence of a single sample. Thus, (ϵ, δ) -DP constrains the privacy risk for a mechanism by ϵ , with δ being the probability that the privacy does not hold.

An important property of DP is given by the composition theorem, which enables the computation of the privacy cost of multiple applications of DP mechanisms.

Theorem 1 (Composition of DP Mechanisms [14])

Let $\mathcal{M}_i : \mathcal{D} \rightarrow \mathcal{R}_i$ be (ϵ_i, δ_i) -DP for $i \in [k]$. Then if $\mathcal{M}_{[k]} : \mathcal{D} \rightarrow \prod_{i=1}^k \mathcal{R}_i$ is defined to be $\mathcal{M}_{[k]}(x) = (\mathcal{M}_1(x), \dots, \mathcal{M}_k(x))$, then $\mathcal{M}_{[k]}$ is $(\sum_{i=1}^k \epsilon_i, \sum_{i=1}^k \theta_k)$ -DP.

2.4. Differential Privacy for Machine Learning

Abadi et al. [1] transferred the notion of DP to ML. They showed that the privacy cost of each step of optimisation (using stochastic gradient descent (SGD) or another optimiser) can be calculated when performing two additional steps: First, the global L_2 -norm of a batch of gradients is clipped to S , which bounds the sensitivity of the set of gradients. Second, the averaged gradients are noised using Gaussian noise calibrated to the sensitivity with a standard deviation of zS , where z is the noise multiplier affecting the privacy cost of the step. Due to Theorem 1, the privacy spending of multiple consecutive DP optimisation steps can be determined. The so-called *Moments Accountant* [1] was introduced as a mechanism to keep track of the privacy spending over multiple epochs. Given a privacy budget ϵ , the Moments Accountant can then halt the training, when the budget is about to be depleted. In practice, we use a Rényi differential privacy (RDP) [40] accountant for tracking the privacy spending. An explanation of RDP can be found in Appendix B.

2.5. Differential Privacy for Federated Learning

A key reason for using FL is the preservation of data privacy. However, it was shown that the original FL algorithm does not prevent data reconstruction by a malicious client or server [52,57]. Thus, recent FL approaches often use DP to provide formal privacy guarantees.

There are two ways of introducing DP into FL. The first way is LDP which corresponds to the application of DP optimisation by the data owners, as explained above. Thus, all clients are responsible for gradient norm clipping and noising, as well as tracking their own privacy spending. When the local privacy budget is spent, clients are not available for selection by the server anymore.

The other option for DP is FL-specific and called CDP, or sometimes user-level or client-level privacy [18, 38]. Here, the clients only clip the L_2 -norm of their overall model update and send it to the server while the Gaussian noise is added by the server during the aggregation step. This requires trust of the clients in the server, since their model updates are not properly secured, and a malicious server could infer information about private data characteristics.

The DP guarantees for LDP are on a sample level, meaning each data sample is protected, while CDP merely protects the data on a client level.

3. Related Work

Synthetic data generation is an active field of research with related works utilising VAEs [29], generative adversarial nets (GANs) [20], or other statistical approaches. Most papers require a central dataset [2, 5, 11, 16, 25, 32, 36, 47–49, 54], with only a handful using FL in their algorithms [3, 11, 17, 26, 27, 34, 41, 51, 55, 56]. In the following subchapters, we discuss the federated GAN- and VAE-based approaches separately, restricting ourselves to privacy-preserving approaches.

3.1. Data Generation With DP-GANs

The majority of works in the field of differentially-private synthetic data generation use GANs as their core model. GANs consist of a generator and a discriminator model that are jointly trained using a min-max game with conflicting objectives. The discriminator aims to differentiate between real and synthetic samples, while the generator tries to synthesise data that fools the discriminator. The generative capabilities of GANs are very high, with recent GAN architectures being able to synthesise high-quality, realistic image data [6], however, the training procedure requires a lot of data and suffers from several failure modes where the model does not converge.

Jordon et al. [27] transfer the differentially private Private Aggregation of Teacher Ensembles (PATE) framework [42, 43] to GANs. Augenstein et al. [3] developed a CDP algorithm for GANs for the purpose of debugging any issues with client data used for FL. Since the generator training step does not require real data, it is performed by the server and only the discriminator is updated locally by each client. Triastcyn and Faltings [51] describe a similar approach for two clients and additionally propose an alternative DP formulation called Differential Average-Case Privacy. Alternatively, Zhang et al. [56] propose a similar approach to ours for GANs, where only the generator is synchronised using FL. However, the DP updates are performed for the discriminator, so that the DP is only indirectly introduced into the generator. Xin et al. [55] argue that a parallel training setup is inefficient in terms of data access and DP since all selected clients work with an older model in parallel. By instead training the GAN sequentially, clients can build directly on top of the predecessors’ training progress. Zhang et al. [56] transfer DP GAN training to a more complex GAN structure called InfoGAN.

3.2. Data Generation With DP-VAEs

Only three papers and one thesis have investigated the generative capabilities of federated VAEs to synthesise data.

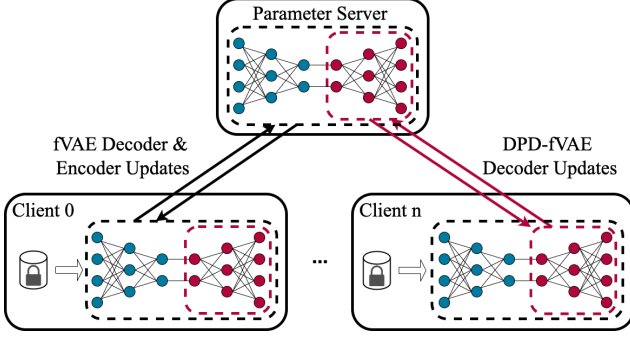


Figure 1. Comparison of vanilla federated Variational Autoencoder (fVAE) and the proposed DPD-fVAE. In the figure, Client 0 is updated using vanilla fVAE, so the complete VAE is exchanged between clients and server. Client n stands exemplary for our proposed method, where only the decoder (red) is updated by the clients. The encoders (blue) are only optimised locally and never leave the sites.

Chen et al. [11] aim to train autoencoders (AEs) and VAEs with strong robustness against three types of attacks. While most of the work is concerned with centralised generator training, one subsection also considers FL (but only for the AE, not the VAE). Alternatively to traditional FL training, Lomurno et al. [34] propose locally training data generators with DP which are then collected on a generator server as a generator pool. This pool is made available for every contributor to synthesise new data from the joint distribution. While being similar to our work in focussing on the generator/decoder component of the VAE, it differs substantially by not aggregating the generators using FL. Jiang et al. [26] worked on an improved LDP algorithm that includes a two-stage dimensionality selection process similar to Liu et al. [31] in order to only aggregate sparse local updates and reduce the privacy cost per step. All the aforementioned papers don't consider CDP in their evaluation, which is likely due to its weaker privacy compared to LDP (user-level privacy instead of sample-level privacy). Georgios [17] covers both types of DP for FL in his thesis and trains conditional VAEs with the capability of generating data for each class. As a limitation, his evaluation uses very high privacy budgets for a simulation on a few clients and argues that scaling up the number of clients would reduce the necessary privacy budget.

4. Federated VAEs with Differential-Private Decoder (DPD-fVAE)

We propose to synchronise only the decoder component of VAEs with FL and DP, while the encoders are kept private and personal. The motivation for this approach is the fact that only the trained decoder is of interest after the training has finished. The encoders are not required to syn-

thesise new data. Fig. 1 illustrates the difference between our proposed DPD-fVAE and vanilla fVAEs. DPD-fVAE can work for CDP or LDP, which we will term C-DPD-fVAE and L-DPD-fVAE, respectively. Algorithm 1 shows our training algorithm for CDP using SGD optimisers for clients and server. Other optimisers can be used accordingly [44]. It is important to note, that stateful optimisers, such as Adam [28] or SGD with momentum, used for the encoder update step keep their state over multiple global rounds, while the decoder optimiser is reinitialised to account for the changes made during FL updates. The algorithm for LDP moves the DP clipping, noising and privacy accumulation to the client update (after line 20). The full algorithm for L-DPD-fVAE can be found in Appendix A.

Algorithm 1 C-DPD-fVAE Training Procedure

- 1: **Input:** client data \mathcal{D}_n for N clients; maximum global rounds T ; client sampling probability q ; local epochs E ; batch size B ; local learning rate η ; privacy budget ϵ , privacy risk δ ; L_2 -norm clip S ; noise multiplier z ;
 - 2: **Server Initialises:** decoder weights θ^0 ; global privacy accountant $\mathcal{M}((\epsilon, \delta), z, q)$
 - 3: **Clients Initialise:** local encoder weights Θ_n
 - 4: **for** $t = 1$ **to** T **do**
 - 5: $\mathcal{C}^t \leftarrow$ randomly select clients with probability q
 - 6: **for** n **in** \mathcal{C}^t **in parallel do**
 - 7: $\Delta\theta_n^t = \text{CDP_CLIENT_UPDATE}(n, \theta^{t-1}, E, B)$
 - 8: **end for**
 - 9: $\Delta\theta^t \leftarrow \frac{1}{qN} (\sum_{n \in \mathcal{C}^t} \Delta\theta_n^t + \mathcal{N}(0, z^2 S^2))$
 - 10: $\theta^t \leftarrow \theta^t + \Delta\theta^t$
 - 11: $\epsilon^t \leftarrow \mathcal{M}.\text{get_privacy_spent}(t, z, q)$
 - 12: **if** $\epsilon^t > \epsilon$ **then**
 - 13: **break**
 - 14: **end if**
 - 15: **end for**
 - 16: **return** θ^t
 - 17: **function** $\text{CDP_CLIENT_UPDATE}(n, \theta, E, B)$
 - 18: $\theta_n \leftarrow \theta$
 - 19: **for** $e = 1$ **to** E **do**
 - 20: **for** local batches $b \in \mathcal{D}_n$, with $|b| = B$ **do**
 - 21: $\theta_n, \Theta_n \leftarrow \text{SGD}(\eta)(\nabla \mathcal{L}(\theta_n, \Theta_n; b))$
 - 22: **end for**
 - 23: **end for**
 - 24: $\Delta\theta_n \leftarrow \theta - \theta_n$
 - 25: $\Delta\theta_n \leftarrow \Delta\theta_n / \max(1, \frac{\|\Delta\theta_n\|_2}{S})$
 - 26: **return** $\Delta\theta_n$
 - 27: **end function**
-

Benefits for DP The privacy spending of differentially-private FL is determined solely by the choice of the noise

multiplier z and, depending on the type of DP, the sampling probability q and the number of global rounds T for CDP, and the batch sampling probability $\frac{B}{|D_n|}$ and local optimisation steps $E \times \lceil \frac{B}{|D_n|} \rceil$ for LDP. Still, the effectiveness of model training can differ immensely depending on the choice of the L_2 -norm clipping parameter S , which additionally affects the standard deviation $\sigma = zS$ of the added Gaussian noise. Having a large S can reduce the number of clipped parameters and thus retain more information, however, it also requires more noise. Too small S values clip too many parameters, hampering good training progress, even if the added noise is smaller. Thus, it is beneficial to have smaller L_2 -norms in the weight updates, allowing for less noise with a sufficiently large number of unclipped parameters. The factors impacting the magnitude of the L_2 -norms in FL are the following: More local training progress in terms of a higher learning rate, an optimiser with momentum, or more local epochs accumulates larger weight updates and thus larger L_2 -norms. Additionally, larger networks with more parameters naturally tend to have larger global L_2 -norms. This highlights the benefit of our proposed approach of only synchronising the decoders, which cuts the number of aggregated model parameters approximately in half (depending on the exact VAE architecture). Thereby, smaller values for S can be chosen which, in turn, reduces the required noise for the same privacy spending. Similarly, for LDP, we can use a non-DP optimiser for updating the encoder parameters, and only clip and noise the decoder’s weights. Firstly, this doesn’t introduce any direct noise into the encoder, and secondly, it again lowers the required noise for the decoder’s DP-optimiser at the same level of privacy guarantee.

As an additional benefit, the smaller number of transmitted parameters also improve the communication efficiency of the algorithm. Since this is not the motivation of our work, we leave an in-depth evaluation to future work.

5. Experiments

5.1. Experiment Setup

Datasets To compare with related work, we evaluate our method on three different image datasets: MNIST [30], Fashion-MNIST [53] and CelebA [33]. The first two consist of 28×28 pixel greyscale images of handwritten digits and clothing articles, respectively, both with ten different classes. There are 60,000 images for training and 10,000 images for testing in both datasets. We distribute the training data in an independent and identically distributed (i.i.d.) fashion across 500 and 100 clients, respectively, resulting in 120, or 600 local samples. We chose two different client numbers to analyse multiple real-world scenarios.

CelebA is a dataset of RGB images of celebrity faces with multiple binary attributes such as facial hair or

glasses associated with them. In our experiments, we use male/female as labels and scale the images down to 32×32 pixels. The distribution of CelebA follows the LEAF framework for benchmarking of FL [8], which groups images by celebrity id, excluding those with less than 5 examples. This results in 9,343 clients with 19.0 ± 7.0 training samples for a total of 177,457 training samples. Approximately 10% of images per celebrity are split off and combined as the central test set with 22,831 samples.

Evaluation Metrics In addition to the subjective visual inspection of synthetic images, all VAE models are evaluated and compared using two widely used metrics. The basis for the metric computations are synthetic datasets of 60,000 images, and we average the scores over five of these datasets.

The first metric is the accuracy of classifiers trained on a synthetic dataset, which shows the utility of the data generator for training ML models. We use a central test set for evaluating the classifiers, and, like related work, we report results for logistic regression, a multi-layer perceptron (MLP) and a convolutional neural network (CNN) [9]. For the specific model architectures, we refer to Appendix C.

Secondly, we report the widely-used Fréchet Inception Distance (FID) [22], which determines the similarity of two image datasets. The FID is calculated by evaluating the Fréchet Distance [13] between the Gaussian distributions of the Inception-v3 [46] network’s feature activations. A lower FID score indicates that the synthetic data more closely resembles the original data in terms of similarity and variability. In our experiments, we compute the FID between the synthetic dataset of 60,000 samples and the complete test set of the datasets.

Implementation We use TensorFlow 2.5.0¹ and TensorFlow Federated 0.19.0² for the FL code. For the accumulation of privacy spending, we use the RDP accountant supplied by TensorFlow Privacy 0.5.2³. The distributed scenario is simulated by parallelising tasks on a single GPU. Our code can be accessed on GitHub⁴. The VAE architectures use CNNs for encoders and decoders, the model specifics can be found in Appendix C. All experiments were performed on either an NVIDIA A100 40GB, an NVIDIA A40 48GB or an NVIDIA RTX Titan 24GB GPU.

Hyperparameter Optimisation For each experiment, we performed a hyperparameter optimisation over a predefined discrete search space. Where the total number of parameter combinations was below 150, we evaluated all of them in

¹www.tensorflow.org

²www.tensorflow.org/federated

³github.com/tensorflow/privacy

⁴github.com/Bjarnepfitzner/generative_fl_tff

Table 1. Results for the non-private variants of fVAE and DPD-fVAE, compared to a VAE trained on a centralised dataset.

Dataset	Model	FID	CNN Acc. (%)
MNIST	Central VAE	28.2	97.0
	fVAE	30.6	96.7
	DPD-fVAE	25.3	97.3
Fashion-MNIST	Central VAE	56.2	82.4
	fVAE	44.6	83.3
	DPD-fVAE	73.3	76.7

a grid search, and used a random search strategy over 100 trials otherwise. An exact overview of the evaluated hyperparameter values can be found in the Appendix D.

Before doing any FL experiments, we evaluated different model architectures, latent dimensions and β values using centralised VAE training. Similarly to Lomurno et al. [34] and supported by [7], we searched β values between zero and one to emphasise image clarity and found that $\beta = 0.01$ performed best. These model and loss hyperparameters were then fixed for all following experiments.

For the non-private experiments, we optimised the batch size B , the number of local epochs E , the client sampling probability q , the clients’ optimiser and learning rate $opt(\eta)$, and the global momentum ρ (for a constant global SGD optimiser with learning rate 1.0).

For the DP experiments, we first defined the DP privacy level in terms of ϵ and δ . In all experiments, we use $\delta = 10^{-5}$ which is commonly used in related work and sufficiently close to the suggested $\frac{1}{|\mathcal{D}|}$ for our datasets. For ϵ , we default to 10.0 but show some results for a low privacy budget of 1.0. We trained the models until the privacy budget ϵ was spent or until a maximum of 1,000 rounds. We optimised the two DP hyperparameters, the L_2 -norm clipping threshold S and the noise multiplier z , in addition to the aforementioned FL hyperparameters.

5.2. Non-Private Training

First, we establish a comparable performance in the non-private case of federated VAE training with only synchronising the decoder, against full VAE synchronisation. Thus, we do not perform any clipping or noising and simply restrict the FL synchronisation step to the decoder component of the VAE. In Tab. 1, we show the results for the CNN accuracy and FID, trained on datasets synthesised by our method (without DP) and fVAE. As a baseline, we also trained the VAEs on a centralised training set.

The performance of our approach is a comparable to vanilla fVAE and centralised VAE training, only performing slightly worse for FashionMNIST. The hyperparameter optimisation showed, that both federated VAE trainings are

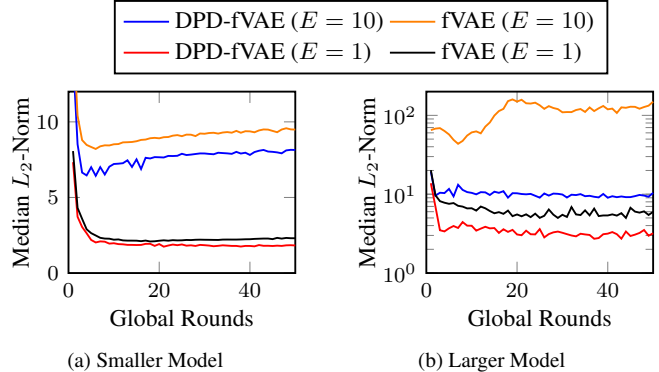


Figure 2. Comparison of the median L_2 -norms in the first 50 global training rounds for FashionMNIST. In Fig. 2a, a smaller model was trained ($\approx 185,000$ variables), while the model in Fig. 2b had more parameters ($\approx 3,850,000$ variables) and uses a log-scale. Note, that both larger models and more local epochs correspond to a larger difference in L_2 -norms.

very robust and achieve good scores across many different combinations. Thus, we conclude, that synchronising only the decoder does not negatively impact the performance of the data generators.

5.3. L_2 -Norm Clipping and Noise Resilience

In preliminary experiments for DP training, we show the improved resilience of DPD-fVAE against central L_2 -norm clipping and added Gaussian noise, the two components of CDP for FL. It should be evident, that the L_2 -norms of the client updates are smaller for DPD-fVAE than for FL with full synchronisation when equating all hyperparameters, which we illustrate in Fig. 2. This effect is increased for more local updates in terms of a higher number of local epochs or a smaller batch size. The difference is also dependant on the size of the network.

Consequently, we can assume a higher resilience against L_2 -norm clipping for DPD-fVAE. We show this in Fig. 3a, where the generated samples for a global L_2 -norm clipping at $S = 0.2$ are a lot clearer using DPD-fVAE compared to vanilla fVAE.

In a second experiment, we investigate the noise resilience of DPD-fVAE. By setting different noise levels (in terms of the standard deviation σ), we compared the resulting synthetic images from both DPD-fVAE and fVAE. In Fig. 3b, we show the results for a noise level of $\sigma = 0.05$ with which DPD-fVAE can still generate comparably clear images, while vanilla fVAE struggles a lot more with the added noise.

5.4. Differentially-Private Training

As the main evaluation of our approach, we investigate the performance of DPD-fVAE for private training of data

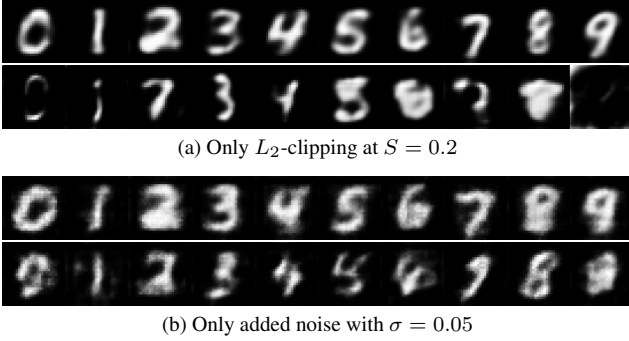


Figure 3. Synthetic images generated by DPD-fVAE (upper rows) and vanilla fVAE (lower rows) either using L_2 -norm clipping (a) or adding Gaussian noise to the global update (b). DPD-fVAE outperforms fVAE in both cases, which together constitute FL with CDP.

generators. We chose to evaluate the CDP scenario using MNIST and CelebA and the LDP scenario using MNIST and Fashion-MNIST. This selection was made based on the number of clients and the amount of local data present for each dataset. For FL with CDP, the privacy cost per global round is largely impacted by the global sampling probability q , with lower q s leading to more possible rounds before the privacy budget runs out. Since the added Gaussian noise is normalised by the expected number of clients per round qN , it is important to have many clients so that q can be chosen to be small, while qN is still large enough.

Similarly for LDP, the local privacy cost depends on the local sampling probability $\frac{B}{|D_n|}$ and the normalisation factor B . Thus, large local datasets are beneficial in this scenario.

MNIST and CelebA are simulated with 500 and 9343 clients, respectively, favouring CDP, while MNIST and Fashion-MNIST possess 120 and 600 local samples, respectively, making them good for LDP.

First, we compare C-DPD-fVAE and L-DPD-fVAE using the MNIST dataset. Fig. 4 shows the data generators’ performances for different levels of ϵ . As expected, smaller privacy budgets result in worse data generators. For our data distribution with 500 clients and 120 local data points, L-DPD-fVAE still outperforms C-DPD-fVAE, however, this could change for different datasets and distributions. Fig. 5 additionally shows images for L-DPD-fVAE with $\epsilon \in 1, 10$.

To illustrate the superiority of DPD-fVAE over vanilla fVAE, Fig. 6 shows images generated based on MNIST using the same hyperparameters for both approaches and LDP. It shows that fVAE fails to converge with the same level of L_2 -norm clipping, whereas DPD-fVAE can generate high-quality images.

Finally, in Fig. 7, we compare synthetic images generated by DPD-fVAE using CDP and LDP for all three datasets. The CelebA images are comparatively noisy be-

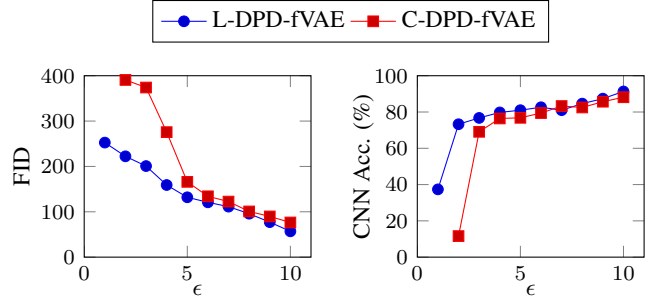


Figure 4. FID and CNN prediction accuracy for different levels of ϵ using L-DPD-fVAE and C-DPD-fVAE.



Figure 5. Synthetic MNIST images generated by L-DPD-fVAE with $\epsilon = 1$ (upper row) and $\epsilon = 10$ (lower row).



Figure 6. Synthetic MNIST images generated by L-DPD-fVAE (upper row) and fVAE with LDP (lower row), following $(10, 10^{-5})$ -DP.



(a) C-DPD-fVAE



(b) L-DPD-fVAE

Figure 7. Synthetic images generated by DPD-fVAE for MNIST, Fashion-MNIST and CelebA using CDP (a) and LDP (b) with $\epsilon = 10$, $\delta = 10^{-5}$.

cause of the data distribution provided by TensorFlow Federated, with clients only having very few images. This makes even non-private FL very difficult. The synthetic dataset still achieves an FID of 261.7 and a CNN accuracy of 69.0, which is in line with related work.

Table 2. Results of the evaluation of $(10, 10^{-5})$ -DP MNIST and Fashion-MNIST models. The best results are indicated in boldface. All related work results are taken from [9], except for DP²-VAE [25], who used a slightly different CNN implementation, making their accuracy not completely comparable.

Method	FL	MNIST				Fashion-MNIST			
		FID	Acc. (%)			FID	Acc. (%)		
			Log. Reg.	MLP	CNN		Log. Reg.	MLP	CNN
Real Data	-	1.1	92.6	97.5	98.9	1.6	84.4	88.3	91.8
G-PATE [35]	✗	177.2	26	25	51	205.8	42	30	50
DP-CGAN [50]	✗	179.2	60	60	63	243.8	51	50	46
DP-MERF [21]	✗	116.3	79.4	78.3	82.1	132.6	75.5	74.5	75.4
GS-WGAN [10]	✗	61.3	79	79	80	131.3	68	65	65
DP-Sinkhorn [9]	✗	48.4	82.8	82.7	83.2	128.3	75.1	74.6	71.1
DP ² -VAE [25]	✗	67.6	85.1	87.0	(90.2)	161.6	77.8	76.0	(76.1)
L-DPD-fVAE	✓	56.9	81.4	81.8	91.3	84.4	75.0	75.4	80.0
C-DPD-fVAE	✓	76.4	79.4	81.1	88.1	N/A	N/A	N/A	N/A

5.5. Comparison with State-Of-The-Art

In Tab. 2, we show the performance of DPD-fVAE on MNIST and Fashion-MNIST together with results reported by related work, following the same structure as in [9, 25]. Our proposed method achieves very competitive scores compared with related work, even though all comparable papers do not consider FL. In our scenario, the local sampling probability for LDP is a lot smaller than for related work, which makes the training task harder (see our motivation in Sec. 5.4). Fig. 8 shows a visual comparison between our results and previous ones for MNIST. For the other datasets, we report more visual results in Appendix E.

We found that most related works using FL for training data generators did not include DP in their evaluation and are thus not realistic for privacy-sensitive, real-world data. The ones that do consider DP [41, 55, 56] did not publish their code and used different datasets, so we could not compare with them. [10] include a section on a federated evaluation of their approach, however, they use a very large and unrealistic privacy budget, and their GitHub repository does not include the FL code for re-evaluation.

6. Conclusion

We propose DPD-fVAE as a novel federated data generation approach which reduces the negative impact of DP on training. Our evaluation has shown the effectiveness of our approach on three different image datasets and across various levels of privacy. Compared with centralised data generation methods, we achieved comparable performance, even if the introduction of FL makes the training task more difficult.

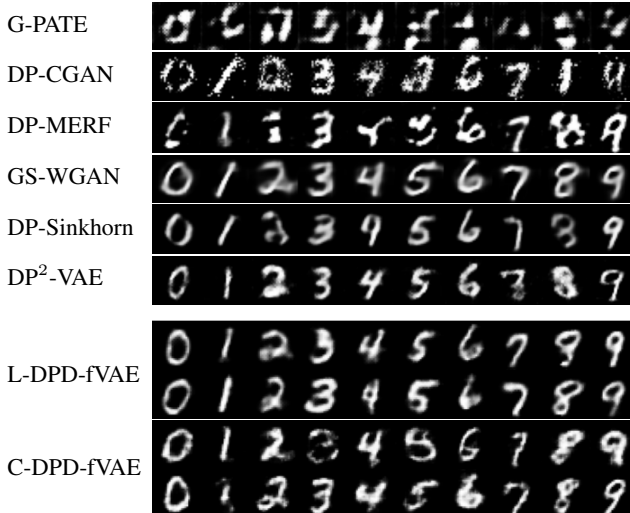


Figure 8. Visual comparison of DPD-fVAE with related work of synthetic MNIST samples under $(10, 10^{-5})$ -DP.

In future work, we aim to investigate the actual resilience of DPD-fVAE against attacks on data privacy. Additionally, we plan to widen our evaluation by considering a larger set of hyperparameters and also including advanced training techniques such as global adaptive optimisation [44] or per-layer clipping. We further want to investigate how DPD-fVAE performs using novel VAE loss functions, such as Soft-IntroVAE [12], or for other dataset modalities such as tabular data or time-series data. Finally, while related works have investigated federated GANs with private discriminators [15, 56], the benefits for DP have not been a focus of these works and would be valuable to analyse.

References

- [1] Martin Abadi, Andy Chu, Ian Goodfellow, H Brendan McMahan, Ilya Mironov, Kunal Talwar, and Li Zhang. Deep learning with differential privacy. In *Proceedings of the 2016 ACM SIGSAC conference on computer and communications security*, pages 308–318, 2016. 1, 3
- [2] Gergely Acs, Luca Melis, Claude Castelluccia, and Emiliano De Cristofaro. Differentially Private Mixture of Generative Neural Networks. *IEEE Transactions on Knowledge and Data Engineering*, 31(6):1109–1121, June 2019. 3
- [3] Sean Augenstein, H Brendan McMahan, Daniel Ramage, Swaroop Ramaswamy, and Peter Kairouz. Generative Models For Effective ML on Private, Decentralized Datasets. Technical report, 2020. 2, 3
- [4] Eugene Bagdasaryan, Omid Poursaeed, and Vitaly Shmatikov. Differential privacy has disparate impact on model accuracy. *Advances in neural information processing systems*, 32, 2019. 2
- [5] Brett K. Beaulieu-Jones, Zhiwei Steven Wu, Chris Williams, Ran Lee, Sanjeev P. Bhavnani, James Brian Byrd, and Casey S. Greene. Privacy-Preserving Generative Deep Neural Networks Support Clinical Data Sharing. *Circulation: Cardiovascular Quality and Outcomes*, 12(7), July 2019. 3
- [6] Andrew Brock, Jeff Donahue, and Karen Simonyan. Large Scale GAN Training for High Fidelity Natural Image Synthesis. Technical report, 2019. 3
- [7] Christopher P Burgess, Irina Higgins, Arka Pal, Loic Matthey, Nick Watters, Guillaume Desjardins, and Alexander Lerchner. Understanding disentangling in β -vae. *arXiv preprint arXiv:1804.03599*, 2018. 6
- [8] Sebastian Caldas, Peter Wu, Tian Li, Jakub Konečný, H. Brendan McMahan, Virginia Smith, and Amee Talwalkar. LEAF: A benchmark for federated settings. *CoRR*, abs/1812.01097, 2018. 5
- [9] Tianshi Cao, Alex Bie, Arash Vahdat, Sanja Fidler, and Karsten Kreis. Don’t Generate Me: Training Differentially Private Generative Models with Sinkhorn Divergence. 2021. 5, 8, 11
- [10] Dingfan Chen, Tribhuvanesh Orekondy, and Mario Fritz. GS-WGAN: A Gradient-Sanitized Approach for Learning Differentially Private Generators. 2021. 8
- [11] Qingrong Chen, Chong Xiang, Minhui Xue, Bo Li, Nikita Borisov, and Dali Kaafar. Differentially Private Data Generative Models. page 18, 2018. 3, 4
- [12] Tal Daniel and Aviv Tamar. Soft-IntroVAE: Analyzing and Improving the Introspective Variational Autoencoder. 2021. 8
- [13] Adrian Dumitrescu and Günter Rote. On the fréchet distance of a set of curves. In *CCCG*, pages 162–165, 2004. 5
- [14] Cynthia Dwork, Aaron Roth, et al. The algorithmic foundations of differential privacy. *Found. Trends Theor. Comput. Sci.*, 9(3-4):211–407, 2014. 2, 3
- [15] Chenyou Fan and Ping Liu. Federated Generative Adversarial Learning. Technical report, 2020. 8
- [16] Lorenzo Frigerio, Anderson Santana de Oliveira, Laurent Gomez, and Patrick Duverger. Differentially Private Generative Adversarial Networks for Time Series, Continuous, and Discrete Open Data, Mar. 2019. 3
- [17] Margaritis Georgios. *Differentially Private Data Synthesis Using Variational Autoencoders*. PhD thesis, 2021. 3, 4
- [18] Robin C. Geyer, Tassilo Klein, and Moin Nabi. Differentially private federated learning: A client level perspective, 2018. 1, 3
- [19] Ian Goodfellow, Yoshua Bengio, and Aaron Courville. *Deep learning*. MIT press, 2016. 2
- [20] Ian Goodfellow, Jean Pouget-Abadie, Mehdi Mirza, Bing Xu, David Warde-Farley, Sherjil Ozair, Aaron Courville, and Yoshua Bengio. Generative adversarial networks. *Communications of the ACM*, 63(11):139–144, 2020. 3
- [21] Frederik Harder, Kamil Adamczewski, and Mijung Park. DP-MERF: Differentially Private Mean Embeddings with Random Features for Practical Privacy-preserving Data Generation. In *Proceedings of The 24th International Conference on Artificial Intelligence and Statistics*, pages 1819–1827. PMLR, Mar. 2021. 8
- [22] Martin Heusel, Hubert Ramsauer, Thomas Unterthiner, Bernhard Nessler, and Sepp Hochreiter. Gans trained by a two time-scale update rule converge to a local nash equilibrium. *Advances in neural information processing systems*, 30, 2017. 5
- [23] Irina Higgins, Loic Matthey, Arka Pal, Christopher Burgess, Xavier Glorot, Matthew Botvinick, Shakir Mohamed, and Alexander Lerchner. beta-vae: Learning basic visual concepts with a constrained variational framework. 2016. 2
- [24] Briland Hitaj, Giuseppe Ateniese, and Fernando Perez-Cruz. Deep Models Under the GAN: Information Leakage from Collaborative Deep Learning. 2017. 1
- [25] Dihong Jiang, Guojun Zhang, Mahdi Karami, Xi Chen, Yunfeng Shao, and Yaoliang Yu. DP 2 -VAE: Differentially Private Pre-trained Variational Autoencoders. 2022. 3, 8, 11
- [26] Xue Jiang, Xuebing Zhou, and Jens Grossklags. Privacy-Preserving High-dimensional Data Collection with Federated Generative Autoencoder. *Proceedings on Privacy Enhancing Technologies*, 2022(1):481–500, Jan. 2022. 3, 4
- [27] James Jordon and Jinsung Yoon. PATE-GAN: Generating Synthetic Data with Differential Privacy Guarantees. page 21, 2019. 3
- [28] Diederik P. Kingma and Jimmy Ba. Adam: A method for stochastic optimization, 2014. 4
- [29] Diederik P Kingma and Max Welling. Auto-encoding variational bayes. *arXiv preprint arXiv:1312.6114*, 2013. 2, 3
- [30] Yann LeCun, Corinna Cortes, and CJ Burges. Mnist handwritten digit database. *ATT Labs [Online]*. Available: <http://yann.lecun.com/exdb/mnist>, 2, 2010. 5
- [31] Ruixuan Liu, Yang Cao, Masatoshi Yoshikawa, and Hong Chen. FedSel: Federated SGD Under Local Differential Privacy with Top-k Dimension Selection. In Yunmook Nah, Bin Cui, Sang-Won Lee, Jeffrey Xu Yu, Yang-Sae Moon, and Steven Euijong Whang, editors, *Database Systems for Advanced Applications*, volume 12112, pages 485–501. Springer International Publishing, Cham, 2020. 4
- [32] Yi Liu, Jialiang Peng, James J Q Yu, and Yi Wu. PPGAN: Privacy-preserving Generative Adversarial Network. 2019

- IEEE 25th International Conference on Parallel and Distributed Systems (ICPADS)*, pages 985–989, Dec. 2019. 3
- [33] Ziwei Liu, Ping Luo, Xiaogang Wang, and Xiaoou Tang. Deep learning face attributes in the wild. In *Proceedings of International Conference on Computer Vision (ICCV)*, December 2015. 5
- [34] Eugenio Lomurno, Leonardo Di Perna, Lorenzo Cazzella, Stefano Samele, and Matteo Matteucci. A Generative Federated Learning Framework for Differential Privacy. 2021. 3, 4, 6
- [35] Yunhui Long, Boxin Wang, Zhuolin Yang, Bhavya Kailkhura, Aston Zhang, Carl A. Gunter, and Bo Li. G-PATE: Scalable Differentially Private Data Generator via Private Aggregation of Teacher Discriminators, Dec. 2021. 8
- [36] Chuan Ma, Jun Li, Senior Member, Ming Ding, Bo Liu, Kang Wei, Student Member, Jian Weng, and H Vincent Poor. RDP-GAN: A Rényi-Differential Privacy based Generative Adversarial Network. Technical report, 2020. 3
- [37] Brendan McMahan, Eider Moore, Daniel Ramage, Seth Hampson, and Blaise Agüera y Arcas. Communication-efficient learning of deep networks from decentralized data. In *Artificial intelligence and statistics*, pages 1273–1282. PMLR, 2017. 1, 2
- [38] H. Brendan McMahan, Daniel Ramage, Kunal Talwar, and Li Zhang. Learning Differentially Private Recurrent Language Models, Feb. 2018. 1, 3
- [39] Luca Melis, Congzheng Song, Emiliano De Cristofaro, and Vitaly Shmatikov. Exploiting Unintended Feature Leakage in Collaborative Learning. page 16, 2018. 1
- [40] Ilya Mironov. Rényi differential privacy. In *2017 IEEE 30th Computer Security Foundations Symposium (CSF)*, pages 263–275. IEEE, 2017. 3, 11
- [41] Vaikkunth Mugunthan, Vignesh Gokul, and Shlomo Dubnov. DPD-InfoGAN: Differentially Private Distributed InfoGAN. *The 1st Workshop on Machine Learning and Systems (EuroMLSys’21), April 26, 2021, Online, United Kingdom*, 1, 2021. 3, 8
- [42] Nicolas Papernot, Martín Abadi, Úlfar Erlingsson, Ian Goodfellow, and Kunal Talwar. Semi-supervised Knowledge Transfer for Deep Learning from Private Training Data, Mar. 2017. 3
- [43] Nicolas Papernot, Shuang Song, Ilya Mironov, Ananth Raghunathan, Kunal Talwar, Úlfar Erlingsson, and Google Brain. Scalable Private Learning with PATE. 2018. 3
- [44] Sashank Reddi, Zachary Charles, Manzil Zaheer, Zachary Garrett, Keith Rush, Jakub Konečný, Sanjiv Kumar, and H Brendan McMahan. Adaptive federated optimization. *arXiv preprint arXiv:2003.00295*, 2020. 4, 8
- [45] Lutz Roeder. Netron, Visualizer for neural network, deep learning, and machine learning models, Dec. 2017. If you use Netron in your research, please cite it using these meta-data. 11
- [46] Christian Szegedy, Vincent Vanhoucke, Sergey Ioffe, Jon Shlens, and Zbigniew Wojna. Rethinking the inception architecture for computer vision. In *Proceedings of the IEEE conference on computer vision and pattern recognition*, pages 2818–2826, 2016. 5
- [47] Tsubasa Takahashi, Shun Takagi, Hajime Ono, and Tatsuya Komatsu. Differentially Private Variational Autoencoders with Term-wise Gradient Aggregation, June 2020. 3
- [48] Uthaiapon Tantipongpipat, Chris Waites, Digvijay Boob, Amaresh Ankit Siva, and Rachel Cummings. Differentially Private Synthetic Mixed-Type Data Generation For Unsupervised Learning, Dec. 2020. 3
- [49] Amirsina Torfi, Edward A Fox, and Chandan K Reddy. Differentially Private Synthetic Medical Data Generation using Convolutional GANs. Technical report, 2020. 3
- [50] Reihaneh Torkzadehmahani, Peter Kairouz, Google Ai, and Benedict Paten. DP-CGAN : Differentially Private Synthetic Data and Label Generation. Technical report, 2020. 8
- [51] Aleksei Triastcyn and Boi Faltings. Federated Generative Privacy. *IEEE Intelligent Systems*, 1672(c):1–1, 2020. 3
- [52] Zhibo Wang, Mengkai Song, Zhifei Zhang, Yang Song, Qian Wang, and Hairong Qi. Beyond inferring class representatives: User-level privacy leakage from federated learning. In *IEEE INFOCOM 2019-IEEE Conference on Computer Communications*, pages 2512–2520. IEEE, 2019. 1, 3
- [53] Han Xiao, Kashif Rasul, and Roland Vollgraf. Fashion-mnist: a novel image dataset for benchmarking machine learning algorithms. *arXiv preprint arXiv:1708.07747*, 2017. 5
- [54] Liyang Xie, Kaixiang Lin, Shu Wang, Fei Wang, and Jiayu Zhou. Differentially Private Generative Adversarial Network. Technical report, 2018. 3
- [55] Bangzhou Xin, Wei Yang, Yangyang Geng, Sheng Chen, Shaowei Wang, and Liusheng Huang. Private FL-GAN: Differential Privacy Synthetic Data Generation Based on Federated Learning. *ICASSP 2020 - 2020 IEEE International Conference on Acoustics, Speech and Signal Processing (ICASSP)*, pages 2927–2931, 2020. 3, 8
- [56] Longling Zhang, Bochen Shen, Ahmed Barnawi, Shan Xi, Neeraj Kumar, Yi Wu, and Boshen Shen. FedDPGAN: Federated Differentially Private Generative Adversarial Networks Framework for the Detection of COVID-19 Pneumonia. 2021. 3, 8
- [57] Joceline Ziegler, Bjarne Pfitzner, Heinrich Schulz, Axel Saalbach, and Bert Arnrich. Defending against reconstruction attacks through differentially private federated learning for classification of heterogeneous chest x-ray data. *Sensors*, 22(14), 2022. 1, 3

Appendices

A. L-DPD-fVAE

We showed the algorithm for C-DPD-fVAE in the main text. The counterpart for LDP is shown in Algorithm 2.

B. Rényi differential privacy

RDP [40] was proposed as an alternative formulation and a natural relaxation of traditional (ϵ, δ) -DP. It is beneficial for the composition of multiple ML optimisation steps with Gaussian noise since the noise scale can be smaller while keeping the same level of privacy compared with (ϵ, δ) -DP. Formally, RDP is defined by:

Definition 2 ((α, ϵ) -RDP [40]) *A randomised mechanism $\mathcal{M} : \mathcal{D} \rightarrow \mathcal{R}$ with domain \mathcal{D} and range \mathcal{R} satisfies ϵ -RDP of order α (or (α, ϵ) -RDP) if for any two adjacent inputs $d, d' \in \mathcal{D}$ it holds that,*

$$D_\alpha[\mathcal{M}(d) \parallel \mathcal{M}(d')] \leq \epsilon, \quad (5)$$

$$\text{where } D_\alpha[P \parallel Q] \triangleq \frac{1}{\alpha - 1} \log \mathbb{E}_{x \sim Q} \left(\frac{P(x)}{Q(x)} \right)^\alpha \quad (6)$$

C. Model Architectures

For all model visualisations we used the Netron tool [45].

C.1. Variational Autoencoders

Our VAE architectures use CNNs as their building blocks. For the MNIST and CelebA datasets, a smaller architecture shown in Fig. 9 performed better, so all presented results are based on that. For Fashion-MNIST, we used a larger VAE architecture that was also used by Jiang et al. [25] and is taken from a public code repository⁵. The exact architecture is shown in Fig. 10.

C.2. Evaluation Classifier

For the evaluation of the usefulness of the synthetic datasets, we use the same three classifiers as Cao et al. [9].

First, we trained a logistic regression (Log. Reg.) with l_2 -regularisation and *lbfgs* solver.

Second, we evaluated a MLP with a single hidden layer with 100 neurons and ReLU activation, and an output layer with one neuron per class and softmax activation.

Finally, we trained a CNN with two convolutional blocks consisting of a 2D-convolution with 32 and 64 kernels, respectively, a kernel size of 3 and stride length 1, followed by a max pooling layer with stride length 2, 50% dropout and ReLU activation. After these blocks, there is another 2D-convolution with 128 kernels and otherwise the same setup

⁵<https://github.com/AntixK/PyTorch-VAE/blob/master/models/cvae.py>

Algorithm 2 L-DPD-fVAE Training Procedure

```

1: Input: client data  $\mathcal{D}_n$  for  $N$  clients; maximum global
   rounds  $T$ ; client sampling probability  $q$ ; local epochs
    $E$ ; batch size  $B$ ; local learning rate  $\eta$ ; privacy budget  $\epsilon$ ,
   privacy risk  $\delta$ ;  $L_2$ -norm clip  $S$ ; noise multiplier  $z$ ;
2: Server Initialises: decoder weights  $\theta^0$ ;
3: Clients Initialise: local encoder weights  $\Theta_n$ ; local pri-
   vacy accountant  $\mathcal{M}_n((\epsilon, \delta), z, \frac{B}{|\mathcal{D}_n|})$ 
4: for  $t = 1$  to  $T$  do
5:    $\mathcal{C}^t \leftarrow$  randomly select clients with probability  $q$ 
6:   for  $n$  in  $\mathcal{C}^t$  in parallel do
7:      $\Delta\theta_n^t = \text{LDP\_CLIENT\_UPDATE}(n, \theta^{t-1}, E, B, \epsilon)$ 
8:   end for
9:    $\Delta\theta^t \leftarrow \frac{1}{|\mathcal{C}^t|} \sum_{n \in \mathcal{C}^t} \Delta\theta_n^t$ 
10:   $\theta^t \leftarrow \theta^t + \Delta\theta^t$ 
11: end for
12: return  $\theta^t$ 
13: function  $\text{LDP\_CLIENT\_UPDATE}(n, \theta, E, B, \epsilon)$ 
14:   $\theta_n \leftarrow \theta$ 
15:  for  $e = 1$  to  $E$  do
16:    for local batches  $b \in \mathcal{D}_n$ , with  $|b| = B$  do
17:       $\Theta_n \leftarrow \text{SGD}(\eta)(\nabla\mathcal{L}(\theta_n, \Theta_n; b))$ 
18:       $\theta_n \leftarrow \text{DP-SGD}(\eta)(\nabla\mathcal{L}(\theta_n, \Theta_n; b))$ 
19:       $\epsilon_n^t \leftarrow \mathcal{M}_n.\text{get\_privacy\_spent}(t, z, q)$ 
20:      if  $\epsilon_n^t > \epsilon$  then
21:        remove  $n$  from client pool
22:      return  $\Delta\theta_n$ 
23:    end if
24:  end for
25:  end for
26:   $\Delta\theta_n \leftarrow \theta - \theta_n$ 
27:  return  $\Delta\theta_n$ 
28: end function

```

as the previous ones, however it is directly followed by a ReLU activation (without pooling and dropout). After that, the output is flattened and fed into another fully-connected layer with 128 neurons and ReLU activation, 50% dropout and a final fully-connected output layer with one neuron per class and softmax activation.

Both neural networks were trained using the categorical cross-entropy loss and an Adam optimiser with a learning rate of 0.001. We additionally used a weight decay of 10^{-4} for all layers, according to the implementation of [9] found on Github⁶.

⁶https://github.com/nv-tlabs/DP-Sinkhorn_code/blob/main/src/train_mnist_classifier.py

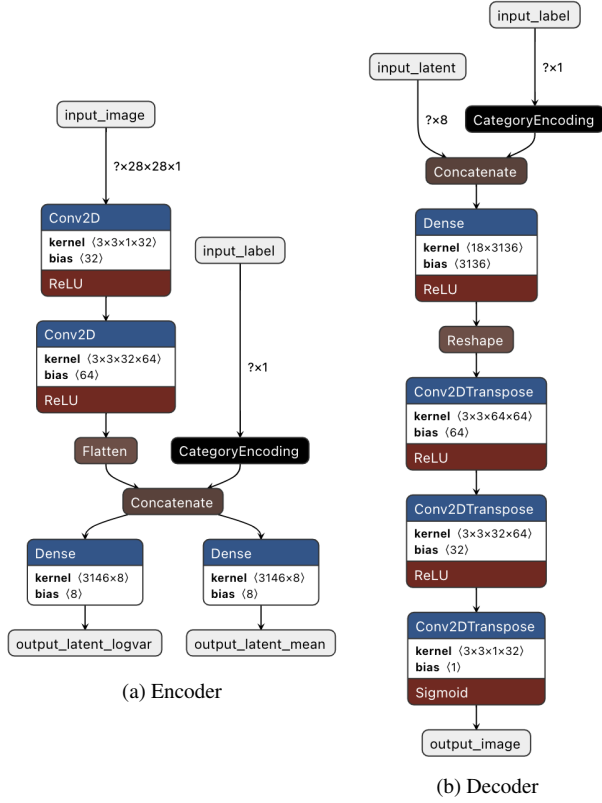


Figure 9. The VAE model architecture for MNIST and CelebA experiments. All convolutional layers have a stride length of 2.

D. Hyperparameters

We investigated a hyperparameter grid with the following options:

$$\begin{aligned}
 \text{local optimiser} &\in \{SGD, Adam\} \\
 \eta &\in \{10^{-2}, 10^{-3}, 10^{-4}, 10^{-5}\} \\
 E &\in \{1, 5, 10\} \\
 \rho &\in \{0.0, 0.5, 0.9, 0.99\} \\
 S &\in \{0.1, 0.2, 0.5, 0.75, 1.0, 1.5, 2.0\} \\
 z &\in \{0.5, 0.6, 0.7, 0.8, 1.0, 1.2, 1.5, 2.0\}
 \end{aligned}$$

Since the datasets were set up with different amounts of local data and numbers of clients, the search space for B and q depends on the dataset. For MNIST and Fashion-MNIST, we chose $B \in \{10, 20, 30, 60\}$, while for CelebA, we chose $B \in \{8, 16, 32\}$. The search space for q was $\{0.01, 0.05, 0.1, 0.2\}$, $\{0.05, 0.1, 0.2\}$ and $\{0.005, 0.01, 0.05\}$ for MNIST, Fashion-MNIST and CelebA, respectively.

We present the selected optimal hyperparameters in Tab. 3.

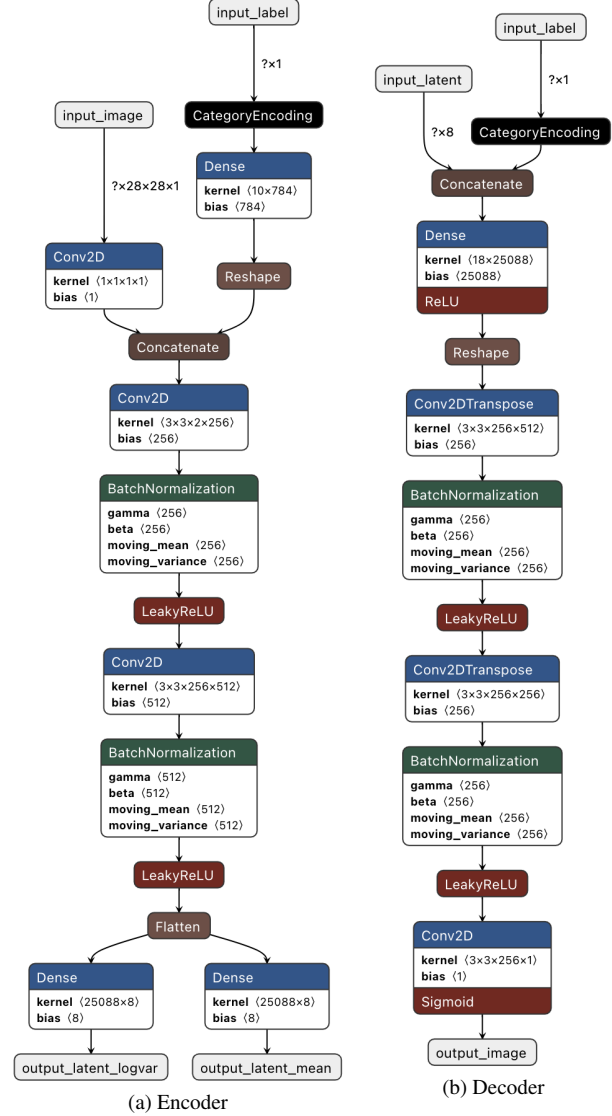


Figure 10. The VAE model architecture for Fashion-MNIST experiments. The first convolutional layer in the encoder and the last one in the decoder have a stride length of 1, for all others, the stride length is 2. The BatchNormalization layers have $\epsilon = 10^{-5}$ and a momentum of 0.9. The LeakyReLU activation uses $\alpha = 0.01$.

E. Additional Results

In Fig. 11, we compare our Fashion-MNIST images with related work. Moreover, we present additional generated images for all datasets and $\epsilon = 10.0$ and $\epsilon = 1.0$ (except for CelebA) in Figs. 12 to 15.

Notably, for training C-DPD-fVAE with $\epsilon = 1.0$ on MNIST, we did not find a well-performing model. This is likely due to the number of clients being 500. Having more clients would allow more global rounds, because smaller q s could be chosen, which reduces the privacy cost per round.

Table 3. Optimal hyperparameters used for generating our results. For all experiments a local *Adam* optimiser performed better than *SGD*.

*For the LDP experiment using MNIST, we did not perform hyperparameter optimisation for fVAE, but used the exact same ones found for DPD-fVAE in order to do a direct comparison.

Dataset	DP	(ϵ, δ)	Model	B	η	E	q	ρ	S	z	
MNIST	-	-	Central VAE	128	10^{-3}	-	-	-	-	-	
			fVAE	30	10^{-2}	5	0.05	0.5	-	-	
			DPD-fVAE	20	10^{-2}	10	0.05	0.5	-	-	
	CDP	$(10, 10^{-5})$	fVAE	10	10^{-4}	10	0.2	0.0	0.5	1.2	
			DPD-fVAE	20	10^{-3}	10	0.2	0.5	1.0	1.0	
	LDP	$(1, 10^{-5})$	DPD-fVAE	10	10^{-3}	10	0.1	0.5	0.5	2.0	
			fVAE*	20	10^{-2}	5	0.01	0.5	0.1	1.2	
			DPD-fVAE	20	10^{-2}	5	0.01	0.5	0.1	1.2	
	-	-	DPD-fVAE	30	10^{-3}	10	0.1	0.5	0.1	1.8	
			LDP	$(10, 10^{-5})$	Central VAE	32	10^{-3}	-	-	-	-
fVAE					32	10^{-3}	10	0.1	0.5	-	-
DPD-fVAE	32	10^{-3}			10	0.1	0.5	-	-		
-	$(1, 10^{-5})$	fVAE	10	10^{-4}	10	0.05	0.0	0.1	0.7		
		DPD-fVAE	30	10^{-4}	10	0.01	0.0	2.0	1.0		
		DPD-fVAE	10	10^{-4}	1	0.01	0.0	0.2	2.0		
CelebA	CDP	$(10, 10^{-5})$	DPD-fVAE	8	10^{-2}	10	0.02	0.9	0.5	0.7	

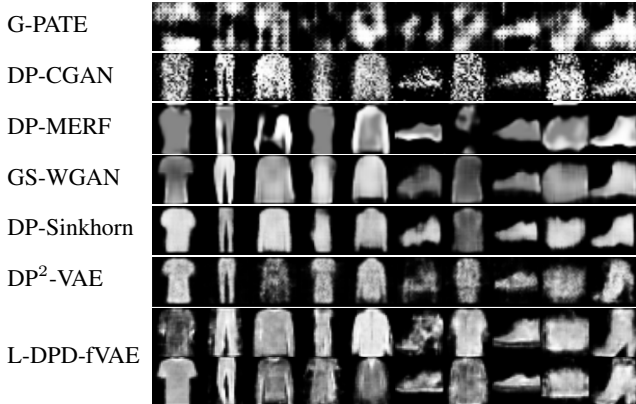


Figure 11. Visual comparison of L-DPD-fVAE with related work of synthetic Fashion-MNIST samples under $(10, 10^{-5})$ -DP.

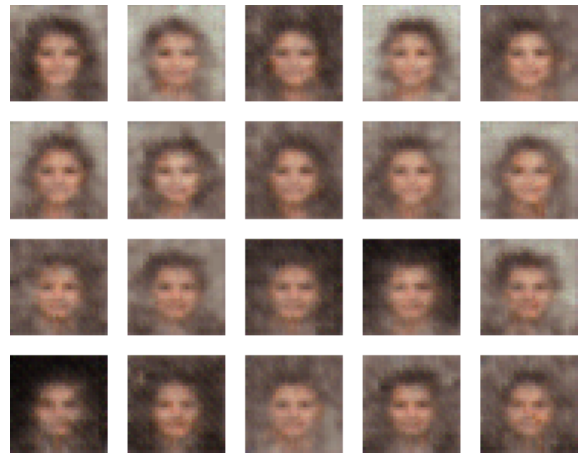


Figure 12. Images generated by C-DPD-fVAE for CelebA with $\epsilon = 10.0$. The upper two rows of images correspond to the female class, the bottom ones to the male class. FID = 261.7.

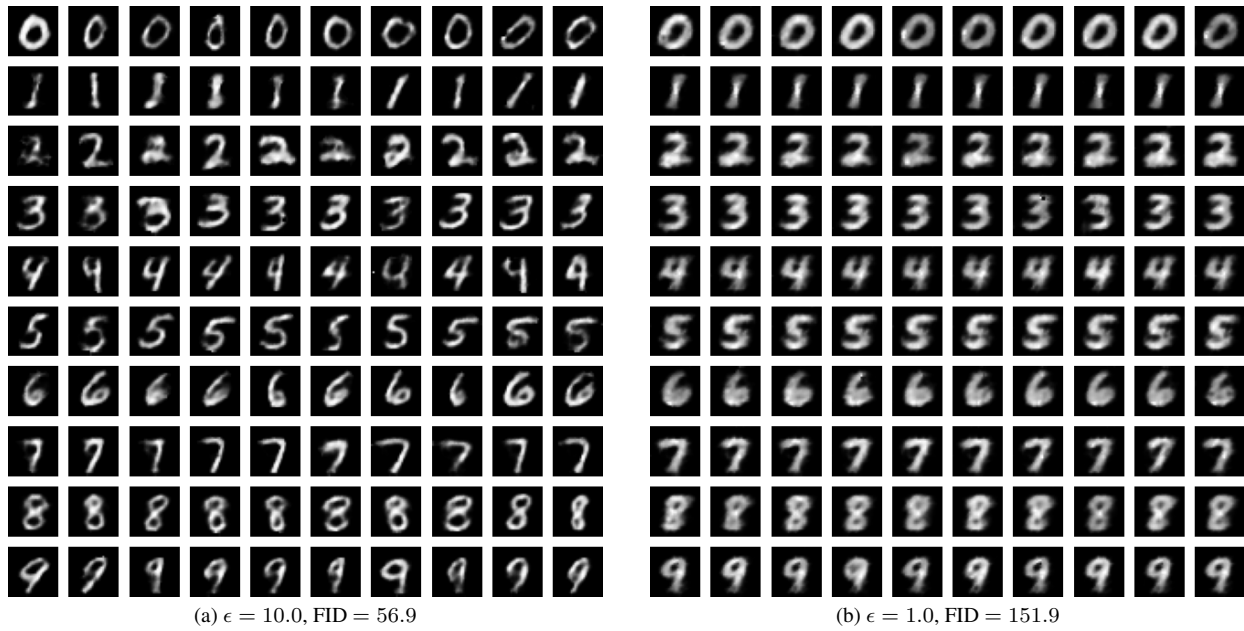


Figure 13. Images generated by L-DPD-fVAE for MNIST with two different privacy budgets.

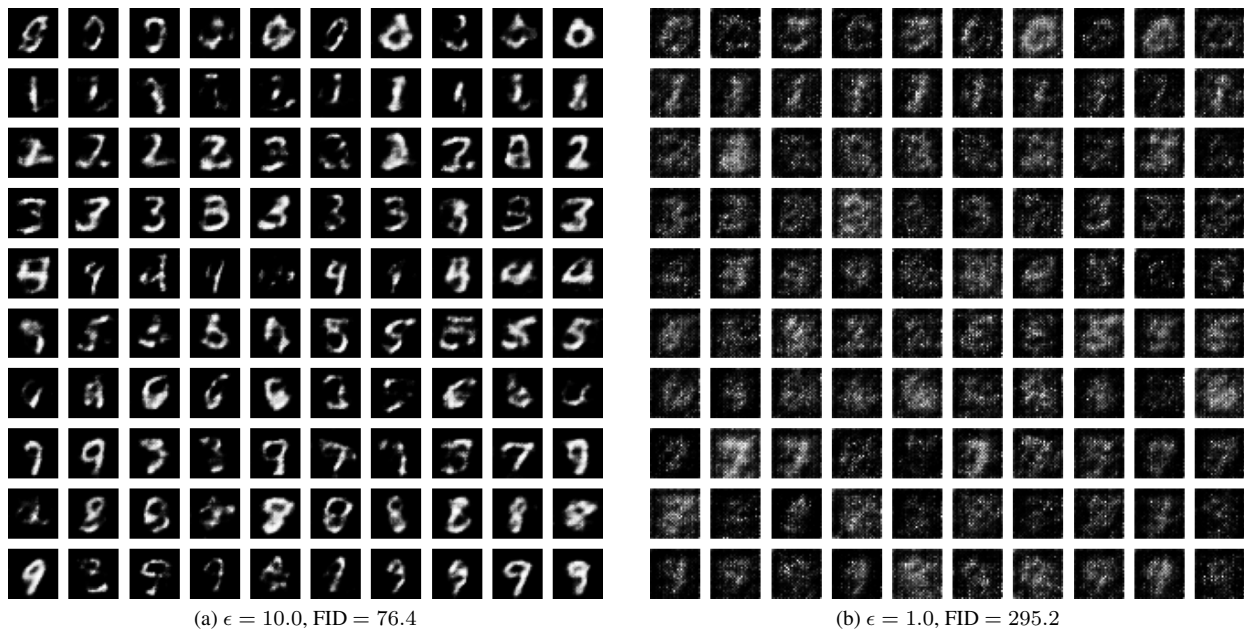
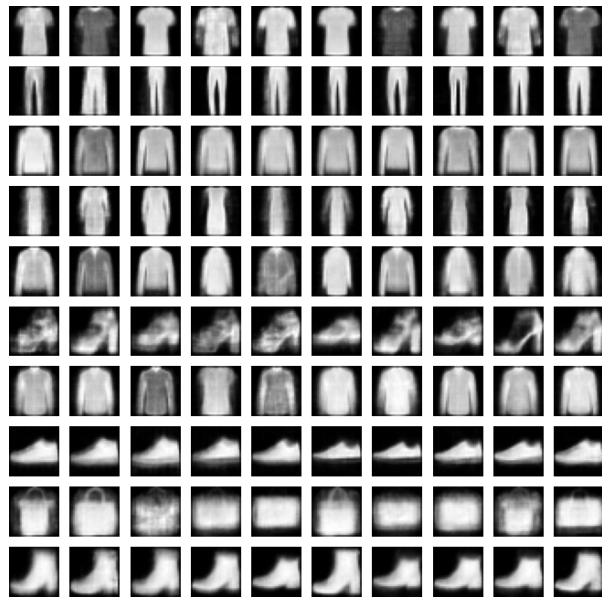


Figure 14. Images generated by C-DPD-fVAE for MNIST with two different privacy budgets.



(a) $\epsilon = 10.0$, FID = 84.4



(b) $\epsilon = 1.0$, FID = 149.8

Figure 15. Images generated by L-DPD-fVAE for FashionMNIST with two different privacy budgets.